PHOTOMASK

BACUS—The international technical group of SPIE dedicated to the advancement of photomask technology.

BACUS NEWS

August 2011
Volume 27, Issue 8

Invited Paper 7985-32

Imaging performance improvements by EUV mask stack optimization

Natalia Davydova, Eelco van Setten, Robert de Kruif, Dorothe Oorschot, and Christian Wagner, ASML Netherlands B.V., De Run 6501, 5504 DR Veldhoven, The Netherlands

Mircea Dusa, ASML Belgium bvba., Kapeldreef 75, 3001 Leuven, Belgium

Jiong Jiang, Wei Liu, Hoyoung Kang, and Hua-yu Liu, Brion Technologies Incorporated, 4211 Burton Drive, Santa Clara, CA 95054, USA

Petra Spies, Nils Wiese, and Markus Waiblinger, Carl Zeiss SMS GmbH, 07740 Jena/64380 Roßdorf, Germany

EUVL requires the use of reflective optics including a reflective mask. The mask contains a reflecting multilayer, tuned for 13.5 nm light, and an absorber which defines the dark areas. The EUV mask itself is a complex optical element with many more parameters than just the mask CD uniformity of the patterned features that impact the final wafer CDU. One of these parameters is absorber height. It has been shown that the oblique incidence of light in combination with the small wavelength compared to the mask topography causes a so-called shadowing effect manifesting itself particularly in an HV wafer CD offset. It was also shown that this effect can be essentially decreased by reducing absorber height and, in addition, it can be corrected by means of OPC.

However, reduction of absorber height has a side effect that is an increased reflectivity of a mask black border resulting in field-to-field stray light due to parasitic reflections. One of the solutions to this problem is optical process correction (OPC) at field edges. In this paper we will show experimental data obtained on ASML EUV Alpha tool illustrating the black border effect and will demonstrate that this effect can be accurately predicted by Brion Tachyon EUV model allowing for a significant cross field CD uniformity improvement with mask layout correction technique.

Also we show by means of rigorous 3D simulations that it is possible to improve the imaging performance significantly by performing global optimization of mask absorber height and mask

Continues on page 3.

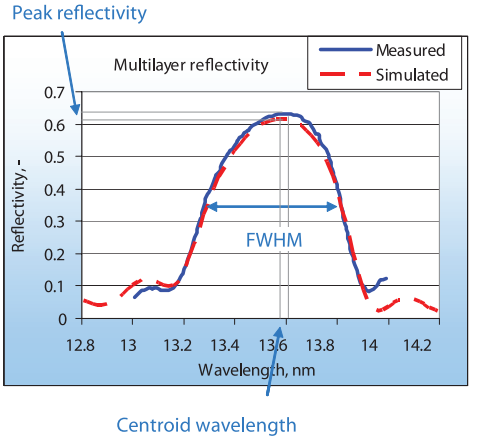

Figure 1. A multilayer stack with 40-layers was optimized in order to match centroid wavelength, peak reflectivity and full width at half maximum (FWHM) of a measured multilayer reflectivity spectrum.

SPIE

EDITORIAL

The Case for Imprint Lithography

Douglas J. Resnick, Molecular Imprints Inc.

The acceleration of the Flash Roadmap over the last three years is nothing short of remarkable. Over the last two years, the combination of 193nm immersion lithography and self aligned spacer double patterning (SADP) has reduced the half pitch by close to a factor of two. Recently, the Intel/Micron NAND joint venture announced a 20nm product. A week later, Toshiba and Sandisk announced a 19nm product. Both have targeted mass production for the second half of this year. The progress is so rapid, the ITRS roadmap for Flash is pulled in every year and still remains behind relative to state of the art production schedules.

This progress literally comes with a price. Double patterning is expensive. As we look beyond 19nm, we face yet another paradigm. At the upcoming half pitches of 16nm and 12nm, double patterning is no longer sufficient and process intensive triple/quadruple self aligned patterning approaches are seriously being investigated. The added process steps introduce critical dimension variations and yet more cost.

Another factor coming into play is the extendibility of NAND Flash. While some are saying that it will be difficult to make stable circuits beyond 12nm, we should recall that optical lithography's death was predicted to occur somewhere around 500nm! Nevertheless, we are likely to hit a wall soon, and 3D memory, such as resistive memory, is being touted as the likely successor. This requires the patterning of even more critical layers, and an even bigger impact on cost.

Alternative solutions, as defined by the ITRS Roadmap include EUVL, multiple beam direct write, self assembly and imprint lithography (and in particular, Jet and Flash Imprint Lithography). First generation EUV tools have been shipped and second generation tools are planned for 2012. Throughput issues caused by insufficient source power, along with the lack of actinic inspection, are potential roadblocks for a NAND solution that is needed as soon as the next two years. Even if these issues are resolved, it is unlikely that the EUV resist will advance fast enough to cleanly resolve 1xnm patterns with a single patterning step. As a result, a double patterning strategy again becomes necessary, negating much of the presumed advantage of cost of ownership.

Multiple beam direct write technology is nowhere near ready for high throughput wafer processing. Self assembly is a complimentary approach and requires another lithographic process to form a template, similar to the 193i SADP methodology. The research is still in its earliest stages and is far away from being ready for insertion into production.

This leaves imprint lithography. There is no question that single patterning is possible. Resolution seems to have no limit and low linewidth roughness has been proven time again. More recently, mix and match overlay of better than 10nm was demonstrated and reported at the SPIE Advanced Lithography Symposium. At the same conference, Toshiba also showed imprint electrical yield data for half pitches down to 24nm that were superior to EUV test data. Finally, SEMATECH reported single wafer imprint defectivity of less than 0.10 defects/cm^2. All of this has been accomplished with resources that are a small fraction of what is put towards the development of the EUV infrastructure.

To unlock of the full potential of imprint lithography, a 1xnm infrastructure for mask writing and mask inspection must be completed. While the electron beam resist needed to pattern the master mask is capable of 12nm resolution, the current shaped beam pattern generators are not optimized for sub-22nm resolution. Electron beam based 1x mask inspection is available today, but the throughput needs to be improved. Mask replication needs to mature as well. Given the extendibility of the imprint lithography, its potential impact on cost of ownership and the accelerated pace of learning over the last year, it makes sense to address the mask infrastructure items that enable a cost effective non volatile memory solution.

BACUS

N • E • W • S

BACUS News is published monthly by SPIE for BACUS, the international technical group of SPIE dedicated to the advancement of photomask technology.

Managing Editor/Graphics Linda DeLano
Advertising Teresa Roles-Meier
BACUS Technical Group Manager Pat Wight

SPIE

P.O. Box 10, Bellingham, WA 98227-0010 USA
Tel: +1 360 676 3290 or +1 888 504 8171
Fax: +1 360 647 1445
SPIE.org
customerservice@spie.org

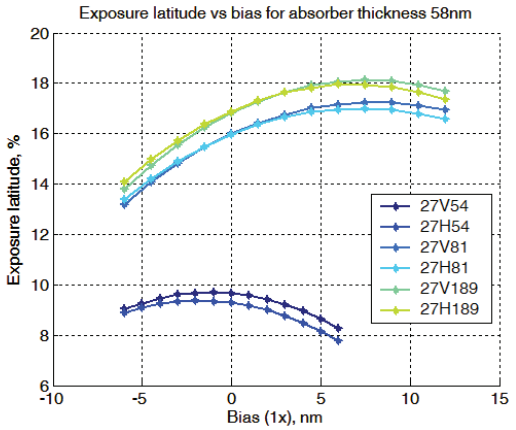

Figure 2. Simulated exposure latitude is shown as a function of mask bias for different LS features for a fixed absorber thickness. NXE:3100 illumination settings are used.

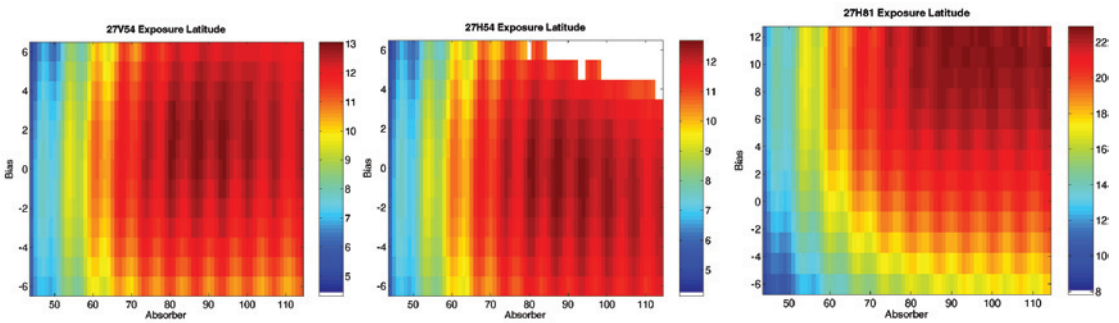

Figure 3. Exposure latitude has a global maximum in bias / absorber thickness space. This maximum is the same for both orientations, but it drifts to larger absorber thicknesses and biases for larger pitches. NXE:3100 illumination settings are used for 27 nm vertical dense lines (left), 27 nm horizontal dense lines (middle), 27 nm horizontal semiisolated lines (right).

bias in order to increase exposure latitude, decrease CD sensitivity to mask making variations such as CD mask error and absorber stack height variations. By sacrificing some exposure latitude throughput of exposure tool can be increased essentially and HV mask biasing can be reduced. For four masks with different absorber thicknesses from 44 nm to 87 nm it is proven experimentally by means of the EUV Alpha tool exposures of 27 nm L/S that the absorber thickness can be tuned to maximize exposure latitude. It was also proven that dose to size grows with absorber height and optimal feature bias depends on mask absorber height.

1. Introduction

EUVL requires the use of reflective optics including a reflective mask. The mask consists of a substrate with ultra low expansion coefficient (ULE), a reflective multilayer that is tuned for 13.5 nm wavelength, and an absorber which defines the dark areas. An EUV mask is a complex optical element with many more parameters that impact the final wafer CDU than the CD uniformity of the patterned features. The multilayer (ML) stack, which typically consists of 40-50 layers of Mo-Si, needs to be tightly controlled for peak reflectivity and centroid wavelength variations. The absorber stack needs to have a uniform and precisely determined height across the wafer to minimize CD errors while taking the flare level from EUV reflection from the absorber into account. Furthermore, the oblique incidence of light in combination with the wavelength that is relatively small compared to the mask topography causes a number of effects which are unique to EUV, such as an HV CD offset and an orientation dependent pattern placement error. These so-called shadowing effects can be corrected by means of OPC, but also need to be considered in the mask stack design. The imaging performance (Exposure Latitude, Mask Error Enhancement Factor) can be optimized by an integral approach, taking the absorber thickness and mask bias into account.

In this paper we will look into the impact of absorber height variations for 27nm dense L/S in resist by means of wafers exposed on an ASML EUV Alpha Tool. Rigorous simulations are performed to evaluate the possibilities for mask stack optimization for the NXE:3100. Furthermore, we will look at the impact of EUV absorber reflectivity on CD uniformity as function of die-spacing and possible correction methods.

2. Global Optimization of Mask Bias and Absorber Thickness

Optimization of absorber thickness for EUV masks is not a trivial task. There exist different figures of merit which can be optimized:

- maximization of NILS/Contrast/Exposure Latitude of features of interest;
- minimization of MEEF;

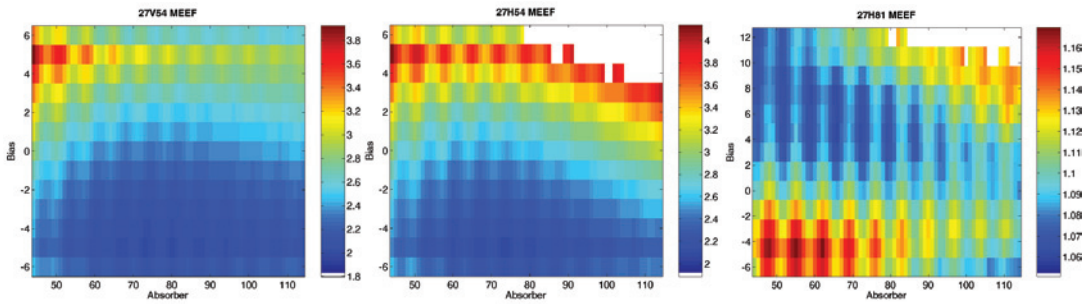

Figure 4. MEEF has a global minimum in bias / absorber thickness space. This minimum is the same for both orientations. NXE:3100 illumination settings are used for 27 nm vertical dense lines (left), 27 nm horizontal dense lines (middle), 27 nm horizontal semi-isolated lines (right).

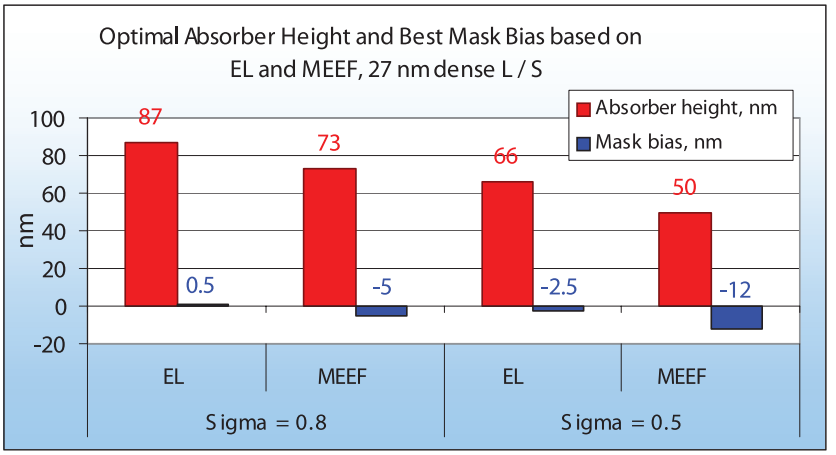

Figure 5. Optimal absorber height and best bias based on exposure latitude and MEEF for two sources: σ=0.8 (corresponds to NXE:3100) and σ=0.5 (corresponds to EUV Alpha tool).

- minimization of CD sensitivity to absorber thickness variations[6];
- absorber thickness reduction to reduce shadowing effect[1,2];
- absorber reflectivity reduction to mitigate the black border effect.

In addition to the figures of merits mentioned above feature bias and dose to size can be optimized in order to improve contrast or increase throughput.

To do these optimizations a rigorous 3D mask simulation was performed in KLA Tencor ProLith X3.2. A multilayer stack with 40-layers was optimized in order to match centroid wavelength, peak reflectivity and full width at half maximum (FWHM) of a measured multilayer reflectivity spectrum. For this purpose thicknesses of two $MoSi_2$ intermixing layers were optimized. The resulting ML stack has the following thicknesses: 2.798 nm Si, 1.448 nm $MoSi_2$, 0.992 nm Mo and 1.786 nm $MoSi_2$. The accuracy of the matching was ~0.01 nm for centroid wavelength, 1.7% for peak reflectivity and <0.001 nm for FWHM. For absorber material measured optical constants were used.

NXE:3100 ASML EUV lithography tool and ASML EUV Alpha tool illumination settings were used for simulations. The settings are NA=0.25 and Sigma = 0.8 (NXE:3100) and Sigma = 0.5 (the Alpha tool) for conventional illumination with discrete pupil source.

Exposure latitude (EL) was used as a metric for bias optimization and it was calculated based on a calibrated full physical resist model. Figure 2 shows that EL is a quadratic-like function of mask bias and therefore can be maximized.

In addition, exposure latitude is a function of both absorber thickness and feature bias and has a global maximum. This maximum is the same for both orientations, but it drifts to larger absorber thicknesses and biases for larger pitches. Simulations show a much smaller exposure latitude for dense LS and thus absorber height variations is optimized based on dense structures. However it is not necessarily the case in reality as we see in experimental data (Figure 15). Therefore logic layers containing more isolated structures may require thicker masks than memory layers.

Mask Error Enhancement Factor (MEEF) has also a global minimum in bias/absorber space and can also be used as optimization metric (Figure 4). As well as EL, MEEF is especially critical for dense structures. MEEF and EL optimizations result in different optimal bias/absorber height combinations. In particular, the MEEF optimization gives ~5nm smaller optimal biases and smaller absorber heights (Figure 5).

Quite unexpectedly, for smaller Sigma=0.5 (the Alpha tool illumination settings) optimal exposure latitude is reached for thinner absorber (conform results in[2]), i.e. counter-intuitively, masks should be thicker for NXE:3100 than for Alpha tool. This result must be confirmed by more extensive simulations and experimental data.

In general, absorber height optimization must include a detailed budget of a particular lithographic process in order to determine

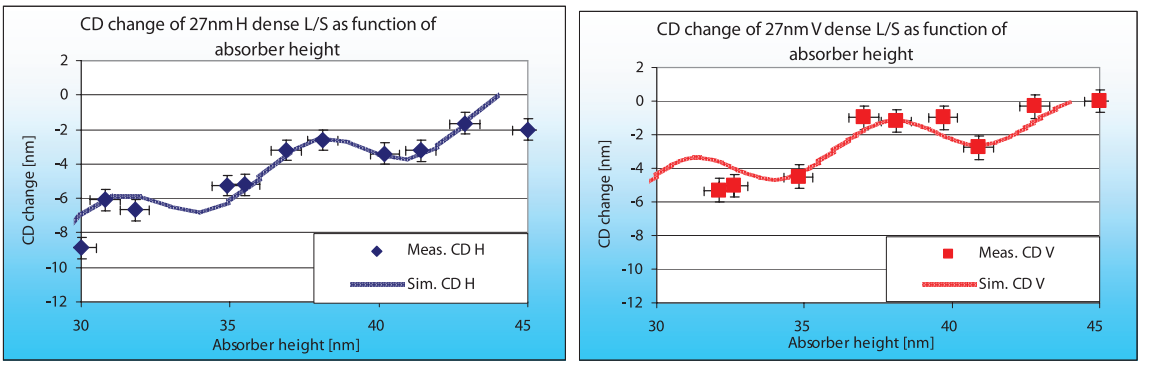

Figure 6. Comparison between simulations and experimental data of the CD change as function of absorber height for 27nm L/S: (left) Horizontal L/S, (right) Vertical L/S.

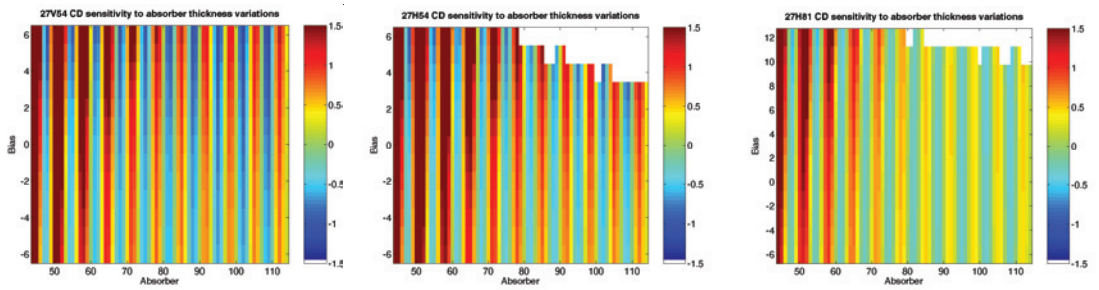

Figure 7. CD sensitivity to absorber height variations oscillates with a period of half-wavelength (13.5/2) through absorber height and (almost) independent on mask bias. NXE:3100 illumination settings are used for 27 nm vertical dense lines (left), 27 nm horizontal dense lines (middle), 27 nm horizontal semi-isolated lines (right).

relative importance of mask CD and absorber height errors, line width roughness, contrast, shadowing errors etc.

3. Optimization of Absorber Height Sensitivity and Absorber Reflectivity

The CD sensitivity as a function of the absorber height variation is also an important parameter in CDU budget. We have investigated[6] the impact of absorber height variations at mask level on the CD at waferlevel experimentally using a dedicated test mask. The mask has a designed absorber height of 44nm lowreflective TaBN and contains 27nm dense L/S grating (at 1x). It was treated with a test stand based on Zeiss MeRiT HR reticle repair tool, thinning the absorber of 10 line sections inside the L/S grating with ~2nm steps by means of a focused electron beam. Consequently the mask was exposed on the EUV Alpha Tool in the IMEC cleanroom facility in Leuven, Belgium. The tool is a full field step-and-scan exposure system with an NA of 0.25 for extreme ultraviolet lithography (EUVL) and is being used for EUVL process development and integration.

The simulated CD as function of absorber height is compared to the experimental data in Figure 6 below. The simulated slope of the curves is ~0.4 (V) – 0.5 (H) nm CD change per nm absorber height change, while the local slope varies between -0.75 and 1.8nm/nm. This means that, depending on the location in the swing curve, small absorber height variations can result in significant CD errors on the wafer, comparable to CD errors from line width variations on the mask. It also means that absorber height must be preferably chosen such that CD sensitivity to absorber height variation is minimal (zero).

Absorber height sensitivity is practically independent of bias and only influenced by absorber height (Figure 7). It swings perfectly in phase for all feature orientations and pitches, but it does not swing in phase with absorber reflectivity (Figure 8). The global optimal absorber heights (Figure 5): 66 nm, 73 nm, 87 nm correspond to low absorber height sensitivities. But at the same time they are close to local reflectivity peaks and therefore mask with this absorber thickness can have relatively large EUV leakage through absorber areas.

4. Compensation of Black Border Reflection Effect

It is known that the reducing of absorber height can essentially reduce shadowing effect.[1] However, this reduction has a side effect that is an increased reflectivity of absorber, in particular in mask black border areas, that is a 2-3 mm wide absorber area around the image field serving as shield from field-to-field stray light. The increase of the absorber reflectivity results in higher amount of the field-to-field stray light due to parasitic reflections.[2,3] As we have also shown EL-optimized absorber thicknesses correspond to relatively high values of absorber reflectivity.

To prevent a CDU impact from field-to-field flare, the mask black border should have very low EUV reflectivity (< 0.2%), which can only be achieved by absorber stack optimization (for example, using a very thick absorber), a special coating, double absorber technique or etching away the entire ML in the black border area, as suggested in [4,5]. However, the CD impact can also be minimized by means of OPC, using information about exposure tool geometry and layout and also knowledge of absorber stack reflectivity. The result of this model as implemented in Brion's Tachyon NXE model

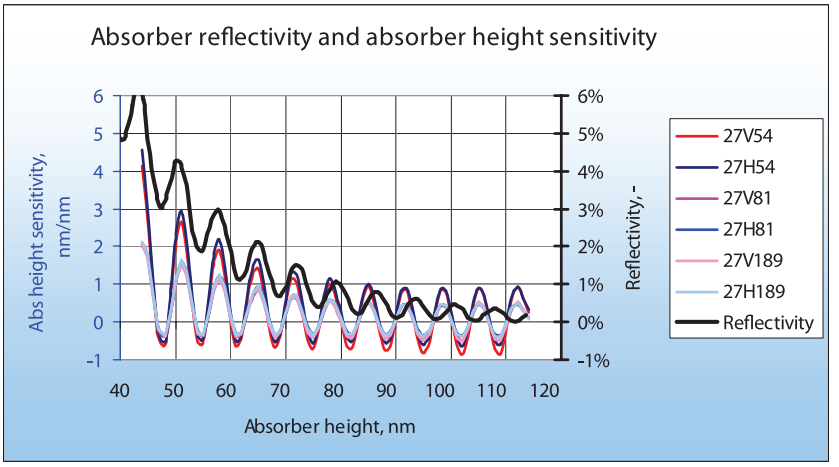

Figure 8. Swing curves of absorber reflectivity and absorber height sensitivity.

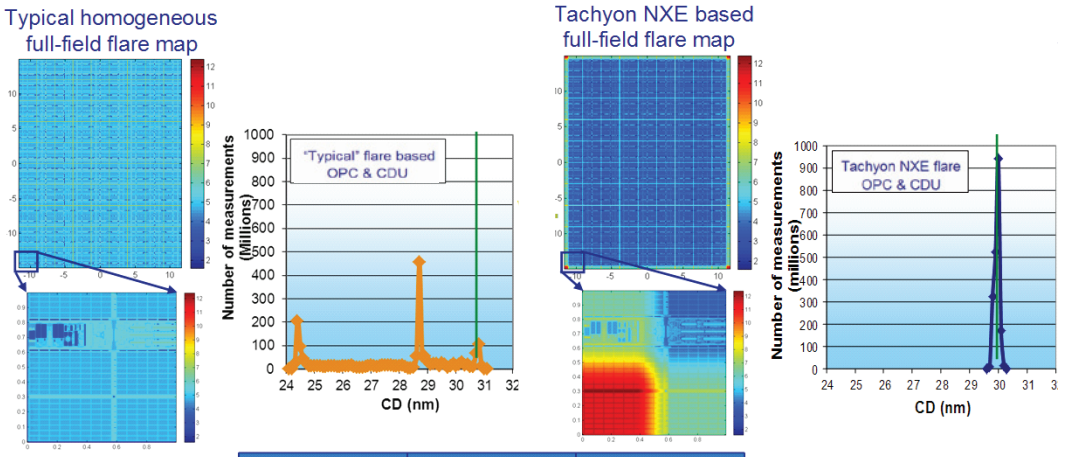

CD statistics	Typical OPC	Tachyon NXE OPC
Mean error (nm)	2.2	0
Sigma (nm)	2.1	0.1
Range (nm)	7.1	0.4

Figure 9. Simulated CDU including field boundary CD errors due to mask black border reflections with and without flare model that takes mask reflections into account. The 'NXE:3100 flare aware' model is found to reduce the impact of mask black border reflections adequately.

is shown in Figure 9. The simulated impact of EUV reflections in the mask black border area is found to be well correctable using an 'exposure tool' aware model, which was the TWINSCAN NXE:3100 in this case.

We have experimentally demonstrated[6] the absorber reflection effect on an ASML EUV Alpha tool. A 44 nm thin absorber mask was exposed in such a way that fields on a wafer were placed at a varying distance from 0 to 3 mm from each other. We have shown that CD of 32 nm dense lines dropped from 32 nm to 24 nm for field to field distances from 0 to 250 micron. Then CD gradually increases over a distance of 250 to 550 micron to reach the target CD value (Figure 10). The transition region is the area where light intensity drops and mask blades have a half-shadow.

The effect is successfully simulated, as shown in Figure 10, by the Tachyon EUV model. The HV offset is expected and caused by mask shadowing. The maximal model to simulation error is 1.5 nm. Notice that with a height of 44 nm, the absorber is a very thin with high reflectivity estimated to be 3-5% absolute. Typical absorbers have reflectivity of less than 1%. Therefore the model error will be reduced to 0.5 nm or lower which is acceptable contribution to OPC budget.

By means of rigorous 3D-mask simulations of the 44 nm absorber stack, we were able to simulate this effect using a 2-pass exposure in ProLith X3.2 (Figure 11) for dense and iso-lines, therefore proving that this is indeed an EUV absorber leakage effect. For simulation a full-calibrated resist model and litho-tool data (aberrations, source pupil, flare) were used.

Also we have compared CD drop due to Black border reflection simulated by the rigorous ProLith model and the Tachyon model for dense and iso-lines and found that for iso-lines the effect is better reproduced by the Tachyon model (Figure 11, Right). Also impact on isolated 2-bar structures was calculated in Tachyon, which was skipped in ProLith because of lack of computing resources on available facilities.

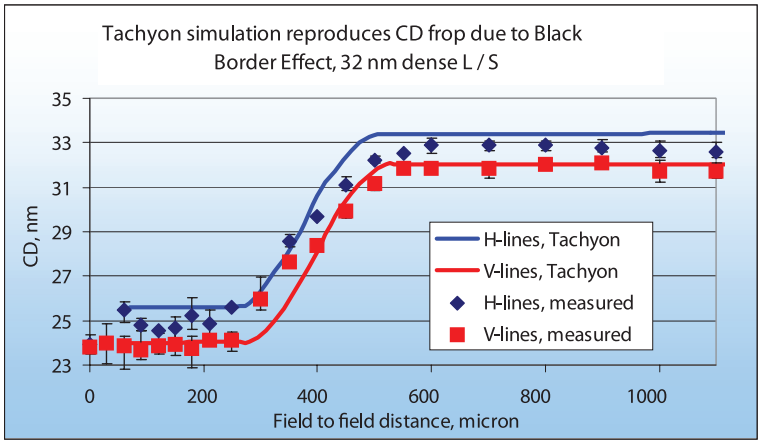

Figure 10. Tachyon simulation of Black border reflection effect demonstrating good modeling capabilities of Tachyon EUV model, allowing for OPC compensation of the Black border effect.

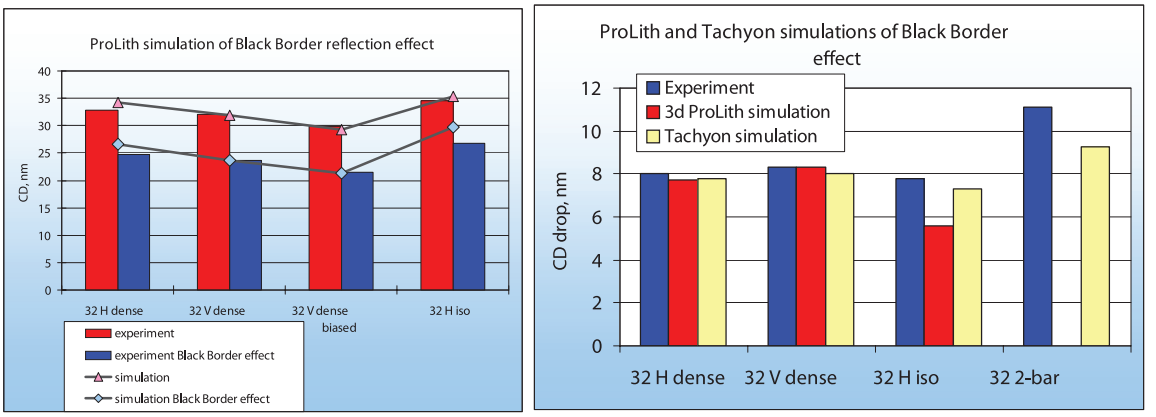

Figure 11. (Left) ProLith 3D mask rigorous simulation of Black border effect compared to the experimental data. (Right) Black border effect simulated in ProLith and in Tachyon.

5. Integral Approach to Absorber Height and Bias Optimization

In order to combine all figures of merit in one procedure, EL-based bias optimization described above is performed for each value of absorber height. Figure 12 shows swing curves of different metrics for optimal bias per absorber height. All metrics have swinging behavior with approximate period of half of EUV Tachyon simulation reproduces CD frop due to Black Border Effect, 32 nm dense L/S wavelength 13.5 nm through absorber thickness. They all swing in phase for features with different pitch and orientation. Though there are varying phase shifts between different metrics since period of oscillations is not exactly half of the wavelength (Figure 13).

Exposure latitude for both orientations has the same level, while HV bias grows with absorber thickness as expected due to shadowing effect. For dense vertical lines optimal bias is negative for thinner absorbers, the behavior is similar to a phase-shifting attenuated mask in ArF lithography. This bias is positive for thicker absorber like for a binary mask. Horizontal lines have negative bias through almost complete range of absorber thicknesses. Semi-isolated and isolated features have large positive biases. Dose to size grows through absorber height (relative dose values are shown in the graph in Figure 12).

Some wild values of best bias and dose to size for large absorber heights have to do with a lack of data at the edge of simulation region. In general, more detailed simulation range of bias and absorber values is needed for an accurate optimization as well as application of advanced optimization techniques based upon theoretical knowledge of CD behavior through absorber height, bias and dose.

Though global optimum for EL lies at 87 nm, one can sacrifice some exposure latitude in order to increase EUVL tool throughput. For example, choosing 54 nm absorber thickness reduces EL by 23% keeping it at acceptable level of about 10% for dense lines while reducing dose to size and increasing throughput by 32%. In addition, it decreases mask HV bias from 2 nm to less than 1 nm.

6. Experimental Determination of Best Bias

Following the EL-based optimization methodology, best bias was determined experimentally for four masks with different absorber thicknesses: 44 nm, 55.4 nm, 58 nm and 87 nm.

The masks were exposed on the EUV Alpha tool at IMEC on wafers coated with 50 nm Shin-Etsu SEVR- 140 resist. Exposure

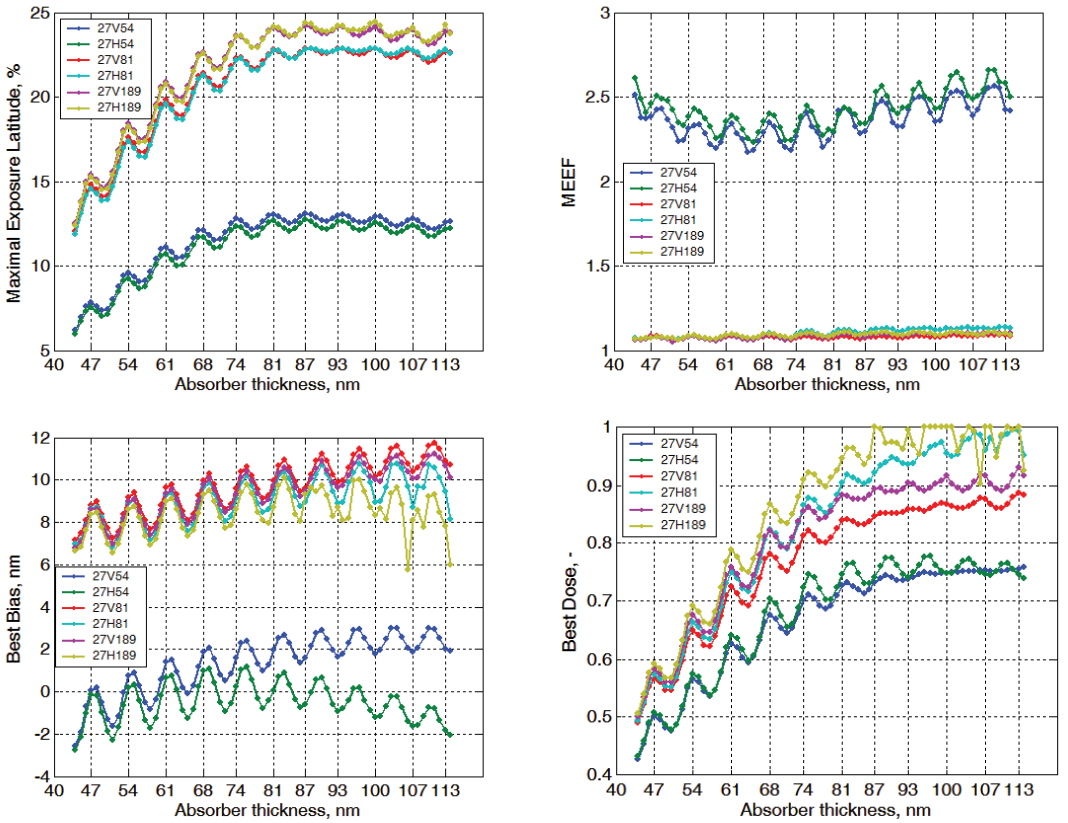

Figure 12. Maximal exposure latitude, best bias, corresponding MEEF and dose to size are shown through absorber thickness for 27 nm dense, semi-isolated and isolated lines. NXE:3100 illumination settings.

latitude and dose to size for a range of biases for 27 nm dense, semi-dense and isolated lines and 32 nm dense lines were measured (Figure 15):

- 44 nm absorber mask: bias range is -5 nm to 5 nm (1x) for all features, dose range is from 6.9 mj/cm^2 to 10.1 mj/cm^2;
- 55.4 nm and 58 nm absorber masks: bias range is ±5 nm around design bias which is 0 nm and 4 nm for vertical dense and (semi-) isolated lines and HV bias is -2 nm for all features, dose range is from 8.5 mj/cm^2 to 12.5 mj/cm^2;
- 87 nm absorber mask: bias range is -5.25 nm to 5.25 nm for dense lines and -7.25 nm to 11.75 nm for isolated lines; dose range is from 13.5 mj/cm^2 to 18.5 mj/cm^2.

Simulations for the Alpha tool illumination setting (Sigma = 0.5) show a pronounced downward trend of exposure latitude, especially for dense lines, and a large HV bias of -3 nm for 87 nm absorber (Figure 14).

For analysis of the experimental data measured mask CD's were used wherever available. There is a near linear relation observed between bias and dose to size; therefore exposure latitude can also be represented as a function of the latter (Figure 15). A quadratic function is fitted on experimental exposure latitude points and optimal bias can be determined. It can be done in two ways: either individually for each feature (single feature optimization as we have done for simulated data in the previous sections) or for multiple features at a single dose to size.

Isolated lines print thicker than target for 44 nm masks, they are not considered further in the analysis of this mask. Semi-dense 27 nm lines were not present on 87 nm absorber mask.

Optimal biases are represented in Figure 16. Quite unexpectedly, for all masks but 87 nm, horizontal features with the same bias printed thinner on wafer than vertical lines and the derived HV bias is therefore positive. For 87 nm the expected negative HV biasing is observed. For almost all features thicker masks require more positive biasing. However for dense horizontal lines a downward trend is observed. This is in line with the simulated results (Figure 14).

The maximal exposure latitude grows with absorber thickness from 44 nm to 55.4 nm and then drops down for the thickest mask of 87 nm. This trend is also observed in simulations (Figure 14).

The dose to size grows in the complete range of absorber thicknesses as expected. Relative difference in the dose between 55.4 nm and 87 nm absorber masks is 23-25% for 27 nm dense lines and 35-36% for 32 nm dense lines which corresponds to a potential throughput increase up to 30-32% for 27 nm node and 53-56% for 32 nm.

7. Summary

An integral approach to mask absorber thickness optimization is developed based on imaging performance. Exposure Latitude and Mask Error Enhancement Factor can serve as metrics for global optimization of absorber height and mask bias. CD sensitivity to absorber height variation and absorber reflectivity can serve as additional parameters to be taken in optimization. It is shown that sacrificing some exposure latitude in order to decrease dose can improve throughput of the imaging tool up to 32% and reduce HV mask bias to less than 1 nm. Simulations indicate that maximal

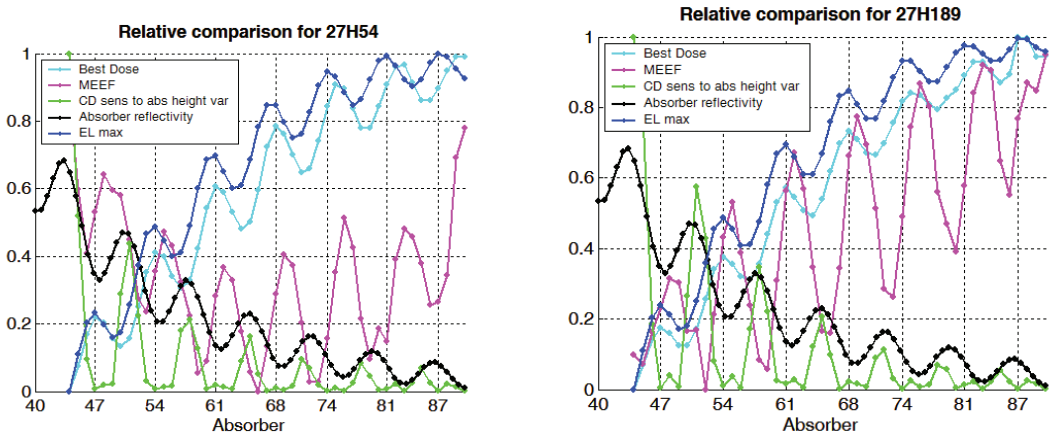

Figure 13. Comparison of phase shifts between normalized swing curves of different metrics for optimal bias calculated per absorber thickness. NXE:3100 illumination settings.

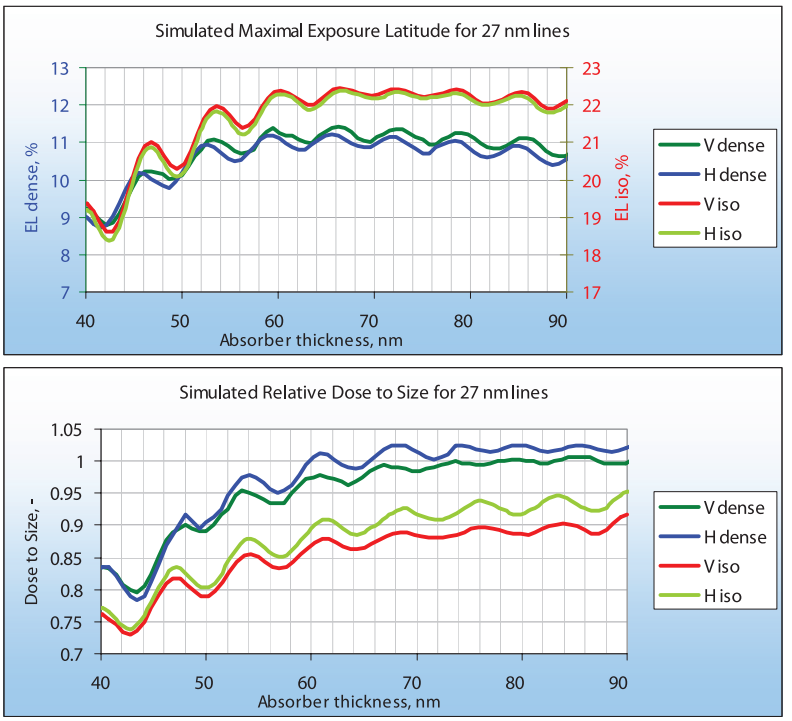

Figure 14. Simulated Best Bias (upper), maximal exposure latitude (middle) and dose to size (bottom) for 27 nm dense and iso-lines. EUV Alpha tool illumination settings (Sigma = 0.5).

exposure latitude is reached for thicker masks (87 nm for σ=0.8) for NXE:3100 illumination than for Alpha Demo Tool (66 nm for σ=0.5). This trend must be proven experimentally. Also simulations for future exposure tools (NXE:3300) and more advanced illumination settings are required.

It is verified experimentally that exposure latitude reaches an optimum in absorber thickness/bias space. For the given range of absorber thicknesses the optimum is reached for 58 nm absorber mask. Dose to size grows with absorber thickness and reduction of the thickness allows decreasing dose to size by 24% for 27 nm while potentially increasing throughput by more than 30%. For most feature types the best bias becomes more positive for thicker masks, while for 27 nm horizontal lines, an opposite trend is observed. The experimental results are in line with simulated trends.

By means of rigorous 3D mask simulation it was confirmed that a field to field flare effect was caused by EUV absorber leakage from mask black border. It is proven that Brion Tachyon EUV model is able to predict and compensate the black border effect by means of mask OPC. Knowledge of absorber EUV reflectivity and geometry of exposure tool is needed for that.

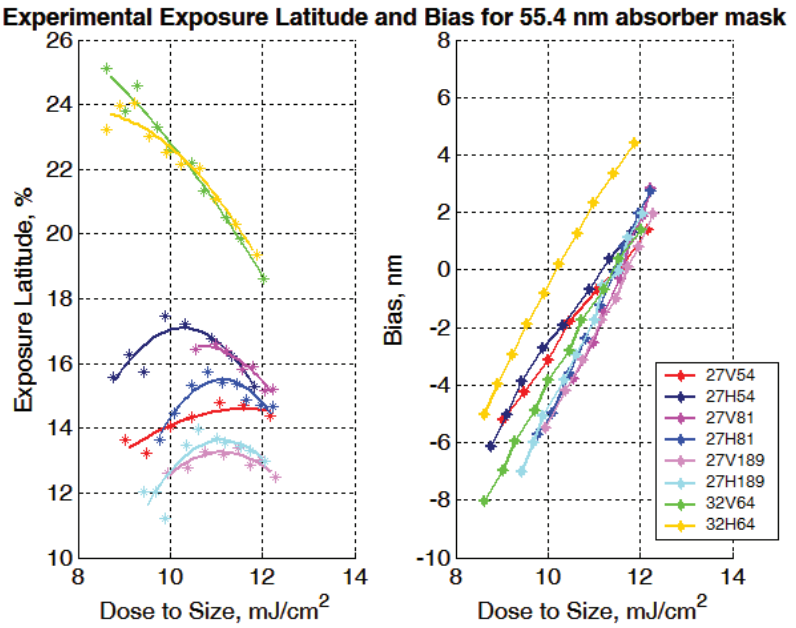

Figure 15. Experimental exposure latitude is shown as a function of mask bias and dose to size. Maximal exposure latitude can be determined per feature or for a single dose for all features at the same time.

8. Acknowledgements

The authors would like to thank ASML ADT team at IMEC and, in particular, Andre van Dijk for exposure support. We thank Vicky Philipsen and Eric Hendrickx for providing an ADT exposed wafer for analysis. We thank Yin Fong Choi for extensive SEM measurements.

9. References

1. E. van Setten et al, Impact of mask absorber on EUV imaging performance, Proc. SPIE, Vol. 7545 (2010).
2. H.S.Seo et al, Absorber stack optimization in EUVL masks: lithographic performances in alpha demo tool and other issues, Proc. SPIE Vol. 7636 (2010).
3. Y. Hyun et al, Feasibility of EUVL thin absorber mask for minimization of mask shadowing effect, Proc. of SPIE Vol. 7636 763614-1 (2010).
4. T. Kamo et al, Thin absorber EUV mask with light-shield border of etched multilayer and its lithographic performance, Proc. SPIE Vol. 7748 (2010).
5. T. Kamo et al, EUVL practical mask structure with light shield area for 32nm half pitch and beyond, Proc. of SPIE Vol. 7122 712227-1 (2008).
6. E. van Setten et al, EUV mask stack optimization for enhanced imaging performance, BACUS (2010).

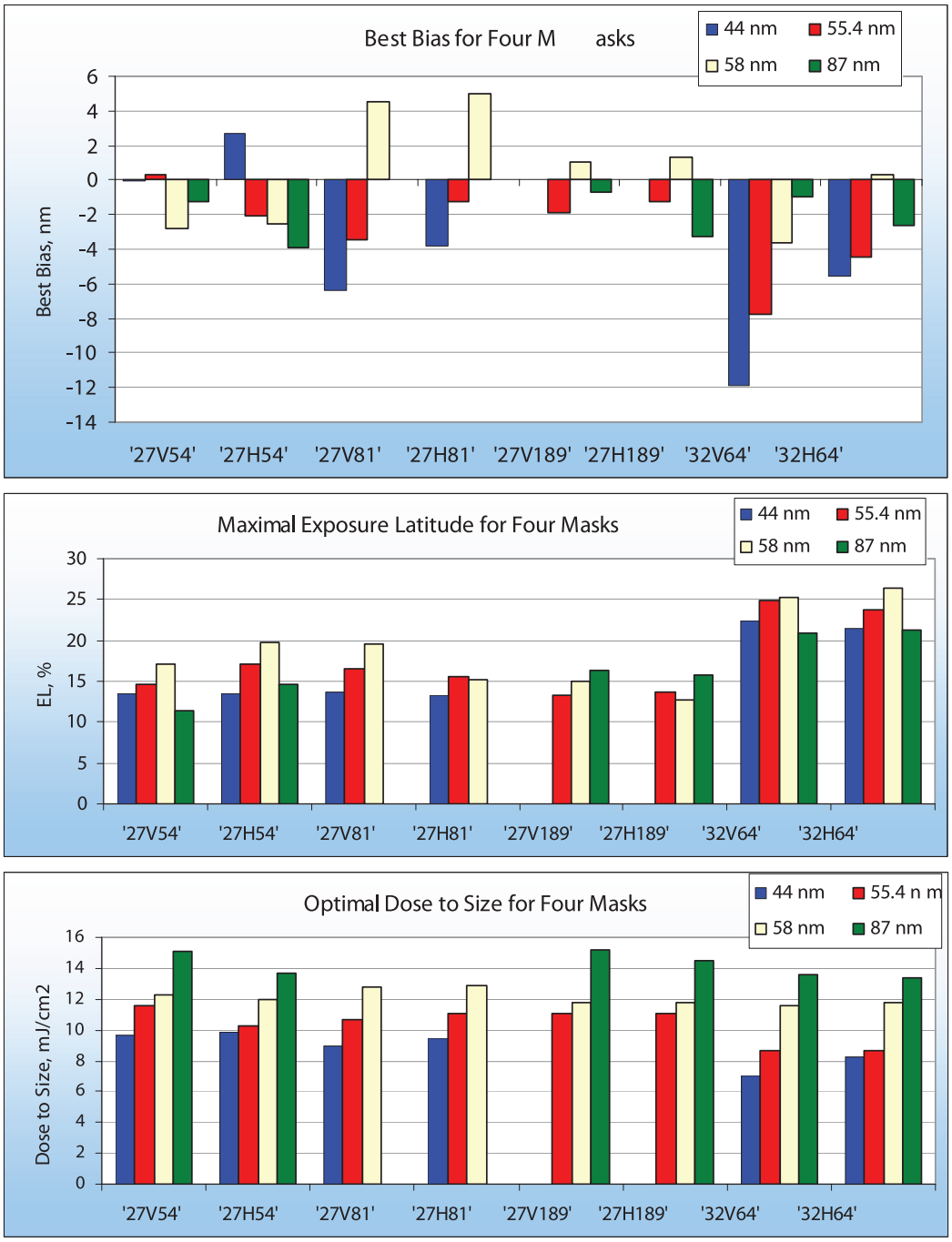

Figure 16. Experimental results for four masks with different absorber thickness: (upper) optimal bias, (middle) maximal exposure latitude, (bottom) dose to size.

Industry Briefs

Continued EUV Progress Towards High Volume Manufacturing

KLA Joins Sematech's EUV Research Program

Semiconductor equipment vendor KLA-Tencor Corp. Tuesday (June 21) joined chip-making vendor consortium Sematech's lithography defect reduction program at the College of Nanoscale Science and Engineering (CNSE) of the University at Albany.

KLA-Tencor will collaborate with Sematech engineers at the defect reduction center for extreme ultraviolet (EUV) tool and materials technology. Specific areas for collaboration include defect source identification and elimination using leading-edge metrology, printability, and characterization methods to advance mask metrology infrastructure and metrology source development, as well as overall EUV manufacturability and extendibility.

Lowering the defect density of EUV lithography is considered critical for inserting it into high-volume manufacturing. The introduction of EUV into high-volume manufacturing has been pushed back several times. EUV lithography is currently projected to be introduced at the 22-nm half-pitch node in 2012 and 2013 at leading IC manufacturers.

"There are too many challenges in moving EUVL to cost-effective manufacturing to solve alone," said Dan Armbrust, Sematech's president and CEO, in a statement. "Increased collaboration with equipment suppliers in the early stages of technological innovation is increasingly required to obtain the breakthrough results that are needed."

IMEC Exposes Wafers on NXE:3100 EUV Tool

Research institute IMEC (Leuven, Belgium) has said it has exposed its first wafers on the NXE:3100 extreme ultraviolet lithography preproduction tool from ASML Holding NV installed at IMEC's pilot fab. The move is a key step towards the adoption of EUV lithography by the chip making industry as the successor to optical lithography.

The ASML NXE:3100 preproduction scanner uses a laser-assisted discharge plasma EUV light source from Xtreme Technologies, a wholly owned subsidiary of Ushio Inc. The tool shows an improvement in throughput and overlay compared to ASML's Alpha Demo Tool (ADT).

The exposure rate of the NXE:3100 is 20 times higher than that of the EUV ADT. The source power is expected to scale to 100 Watts by early 2012, increasing the scanner throughput from the current level to 60 silicon wafers per hour.

A first test of dedicated chuck overlay showed the potential to achieve the smaller than 4-nm target. At the same time, off-axis illumination options have been installed, which at factory acceptance have proven to resolve sub-20nm features using dipole illumination.

The ASML NXE:3100 is interfaced with a Lithius process track from Tokyo Electron Ltd.

Join the premier professional organization for mask makers and mask users!

About the BACUS Group

Founded in 1980 by a group of chrome blank users wanting a single voice to interact with suppliers, BACUS has grown to become the largest and most widely known forum for the exchange of technical information of interest to photomask and reticle makers. BACUS joined SPIE in January of 1991 to expand the exchange of information with mask makers around the world.

The group sponsors an informative monthly meeting and newsletter, BACUS News. The BACUS annual Photomask Technology Symposium covers photomask technology, photomask processes, lithography, materials and resists, phase shift masks, inspection and repair, metrology, and quality and manufacturing management.

Individual Membership Benefits include:

- Subscription to BACUS News (monthly)
- Complimentary Subscription *Semiconductor International* magazine
- Eligibility to hold office on BACUS Steering Committee

spie.org/bacushome

Corporate Membership Benefits include:

- Three Voting Members in the SPIE General Membership
- Subscription to BACUS News (monthly)
- One online SPIE Journal Subscription
- Listed as a Corporate Member in the BACUS Monthly Newsletter

spie.org/bacushome

Calendar

2011

SPIE Photomask Technology

19-22 September 2011
Monterey Marriott
and Monterey Conference Center
Monterey, California, USA
spie.org/pm

2012

Advanced Lithography

12-16 February 2012
San Jose Convention Center and San Jose Marriott
San Jose, California, USA
spie.org/alcall

Submit your Abstracts Now!

You are invited to submit events of interest for this calendar. Please send to lindad@spie.org; alternatively, email or fax to SPIE.

SPIE is an international society advancing light-based technologies.

SPIE

International Headquarters
P.O. Box 10, Bellingham, WA 98227-0010 USA
Tel: +1 888 504 8171 or +1 360 676 3290
Fax: +1 360 647 1445
customerservice@spie.org • SPIE.org

Shipping Address
1000 20th St., Bellingham, WA 98225-6705 USA

SPIE Europe
2 Alexandra Gate, Ffordd Pengam, Cardiff,
CF24 2SA, UK
Tel: +44 29 2089 4747
Fax: +44 29 2089 4750
spieeurope@spieeurope.org • www.spieeurope.org